ELSEVIER

Electrochemistry Communications 4 (2002) 353–357

electrochemistry communications

www.elsevier.com/locate/elecom

# Passivity breakdown of Al 2024-T3 alloy in chloride solutions: a test of the point defect model

Inês T.E. Fonseca [a,*], Nélia Lima [a], João A. Rodrigues [a], M. Isabel S. Pereira [b], João C.S. Salvador [c], Mário G.S. Ferreira [c]

[a] *CECUL, Depto de Química e Bioquímica, Faculdade de Cienias da Universidade de Lisboa, Edificio C8-Campo Grande, 1749-016 Lisboa, Portugal*
[b] *CCMM, Depto de Química e Bioquímica, Universidade de Lisboa, Edificio C8-Campo Grande, 1749-016 Lisboa, Portugal*
[c] *Depto de Engenharia Química, Instituto Superior Técnico, Av. Rovisco Pais, 1049-001 Lisboa, Portugal*

Received 3 January 2002; received in revised form 4 February 2002; accepted 5 February 2002

**Abstract**

Cyclic voltammograms of Al 2024-T3 alloy samples, in deaerated aqueous chloride solutions of various concentrations, have been recorded and analysed.

A linear dependence between the breakdown potential, $E_b$, and the square root of the scan rate, $v^{1/2}$, was found for all chloride concentrations and also for synthetic seawater leading to $\alpha$ values between 0.41 and 0.38.

The breakdown potential at zero scan rate, $E_b$ $(v = 0)$, showed also a good linear dependence on the logarithm of the activity of the chloride anions. From the slope of the straight line a value of 3.29 was obtained for the ratio $(\xi/J_m)$ from which a $\xi$ value less than or equal to $3 \times 10^{15}$ cation vacancies $cm^{-2}$ was calculated.

Average critical concentration of cation vacancies on Al and $\gamma$-$Al_2O_3$ computed from geometric arguments has showed excellent agreement with those computed from experimental data and analytical equations derived from the Point defect model (PDM). © 2002 Published by Elsevier Science B.V.

*Keywords:* Critical breakdown potential; Point defect model; Critical cation vacancies; Al 2024-T3 alloy; Chloride solutions

## 1. Introduction

Al 2024-T3 is a high strength alloy widely used in aerospace applications. This alloy is very sensitive to localised corrosion, particularly in chloride-containing environments, due to its heterogeneous microstructure, which leads to a localised attack mainly, due to galvanic corrosion between copper and intermetallic particles [1,2].

In the literature there are several theories and models, many excellent papers [3–17] and reviews [18–21] on the subject of pitting. However, as much as we are aware analytical equations relating the pitting potential and the scan rate were only derived by Haruna and Macdonald [17] based on the point defect model, PDM.

PDM and associated theories proposed by Macdonald et al. [14–16], provide a theoretical basis for describing the growth and breakdown of passive films on metals and alloys. According to the model the entities involved in the oxide growth are point defects, namely cation, $V_M^{\chi}$ and anion vacancies, $V_O$, giving a defective layer of $MO_{\chi/2}$. The breakdown of passivity induced by anions, e.g. $Cl^-$, has been attributed to the adsorption of the aggressive anions into the surface oxygen vacancies.

$$V_O + X^- \rightarrow X_O. \quad (1)$$

Followed by a Schottky-pair reaction,

$$\text{Null} \rightarrow V_M + (\chi/2)V_O. \quad (2)$$

Thus, anion adsorption would lead to the generation of cation vacancies at the film/solution interface. The enhanced flux of cation vacancies through the film

* Corresponding author. Tel.: +351-21-7500-904; fax: +351-21-7500-892.
*E-mail address:* ifonseca@fc.ul.pt (I.T.E. Fonseca).

1388-2481/02/$ - see front matter © 2002 Published by Elsevier Science B.V.
PII: S1388-2481(02)00273-4

would lead to the growth of a condensate of cation vacancies at the metal/film interface. Once the condensate has grown to a critical size, dissolution of the film at the film/solution interface, and tensile stresses in the barrier layer, induce mechanical and structural instability, resulting in the rupture of passivity leading to localised attack.

During anodic polarisation there is a critical potential at which breakdown occurs. It is generally found that the pitting or breakdown potential depends on the potential scan rate [15,17,22]. Only Macdonald and Haruna [17] give the analytical equations allowing both the scan rate dependence of the breakdown potential and the activity of the aggressive anions.

According to the PDM the critical breakdown potential, $E_b$, for a single breakdown site can be expressed as:

$$E_b\ (v) = (2\xi RT/J_m\chi F\alpha)^{1/2}v^{1/2} + E_b\ (v=0) \tag{3}$$

and

$$E_b\ (v=0) = (2RT/\chi F\alpha)\ln(J_m/J^0u^{-\chi/2}) - RT/F\alpha\ln(a_{x^-}), \tag{4}$$

where $E_b\ (v)$ represents the critical breakdown (pitting) potential for a single site at the scan rate $v$; $\xi$ is the critical concentration of cation vacancies for passivity breakdown and $J_m$ the flux of cation vacancies submerging into the metal phase. $J^0 = D\cdot\hat{a}$, where $D$ represents diffusivity of cation vacancies and $\hat{a}$ the activity of oxygen vacancies; $\chi$ is the stoichiometry of the passive film, $MO_{x/2}$, and the oxidation state of the cation; $\alpha$ represents the dependence of the voltage drop on the applied potential, $E_{appl}$, and $a_{x^-}$ is the activity of the aggressive anions in solution.

Both Eqs. (3) and (4) predict linear relationships. Eq. (3) predicts a linear relationship between the breakdown potential, $E_b$, and the square root of the scan rate, $v$. Eq. (4) predicts also a linear relationship between the breakdown potential, at zero scan rate, $E_b\ (v=0)$, and the logarithm of the activity of the aggressive anions, $a_{x^-}$. The slope of the latter straight line should be higher than $(2.303RT/\alpha F)$, i.e., $> (0.059/\alpha)$ V decade$^{-1}$, at 25 °C). Eq. (4) allows the determination of the parameter $\alpha$, while Eq. (3) allows the determination of the ratio $(\xi/J_m)$. If $J_m$, is known, then the critical concentration of cation vacancies for the rupture of passivity can be estimated.

Under steady-state conditions and for potentials below the critical breakdown potential, $J_m$ cannot be less than the flux of cation vacancies through the passive film, from the film/solution interface to the metal/film interface, i.e. $J_m \geqslant J_{ca}$. Furthermore, $J_{ca}$, the flux of metal cations through the passive film, is given by

$$J_{ca} = i_{ss}N_{AV}/\chi F, \tag{5}$$

where, $N_{AV}$ is Avogadro's number ($6.023\times10^{23}$ mol$^{-1}$) and $i_{ss}$ is the steady-state current density. From experimental polarisation curves, recorded at very low scan rates, the value of the steady-state current can be measured.

## 2. Experimental

Working electrodes (discs of 0.6 cm in diameter) were made with Al 2024-T3 with the composition given in Table 1. Electric contacts were made with silver epoxy, and the disc glued with epoxy resin to the end of a glass tube. The electrodes were first polished mechanically with emery paper down to 600 grit and then given a mirror finish with alumina powders down to 0.3 μm. Finally, the electrodes were washed several times with ultra pure water in an ultrasonic bath to remove residues of alumina powder.

A platinum helix was used as counter electrode, and a commercial saturated calomel electrode connected to the cell via a Luggin capillary was used as reference electrode.

Solutions were deaerated by bubbling $N_2$ from Air Liquid for 30 min.

After each pitting experiment the electrodes were polished to a mirror finish following the procedure already described, in order to remove all the pits and to provide a reproducible surface. For each set of experiments a new electrode was used.

Solutions used were synthetic seawater and neutral deaerated sodium chloride aqueous solutions with concentrations ranging from 0.01 to 1 mol dm$^{-3}$.

A Princeton Applied Research Potentiostat/Galvanostat Model 173 was used in conjunction with a PAR Model 175 Universal Programmer. Cyclic voltammograms were recorded with a Philips PM 8143 X-Y Recorder.

Cyclic voltammograms were always started by holding the electrode for about one minute, at −1.760 V vs. SCE and then sweeping towards positive potentials over the transpassive potential region. The scan rates were varied towards lower values, from 0.250 to 0.020 V s$^{-1}$.

The breakdown potential ($E_b$) was taken to be the intercept (A) of the two lines as shown schematically on the cyclic voltammogram of Fig. 1. The repassivation potential ($E_{repass}$) is also indicated in Fig. 1.

Measurements of the breakdown potential were made at different potential scan rates (0.250–0.020 V s$^{-1}$) and with six chloride concentrations (0.01–1 mol dm$^{-3}$). Duplicates, and sometimes triplicates experiments were performed whenever the differences in the measured breakdown potentials were higher than 10 mV.

Table 1
Composition of the Al 2024-T3 alloy

| | Chemical composition (%) | | | | | | | |
|---|---|---|---|---|---|---|---|---|
| | Cu | Mg | Si | Fe | Cr | Zn | Mn | Al |
| Min. | 3.80 | 1.20 | 0.00 | 0.00 | 0.00 | 0.00 | 0.30 | bal. |
| Max. | 4.90 | 1.80 | 0.50 | 0.10 | 0.10 | 0.25 | 0.90 | |

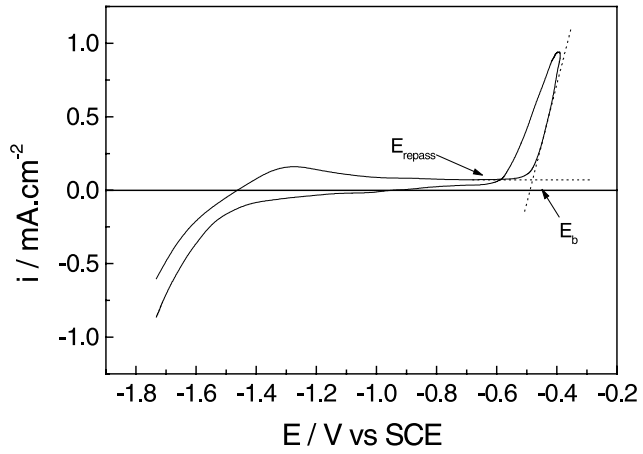


Fig. 1. Method for the determination of the breakdown and repassivation potentials, adapted from Lei et al. [14].

## 3. Results and discussion

Fig. 2 shows two cyclic voltammograms of Al 2024-T3 samples in sodium chloride solutions.

The dependence of the breakdown potential ($E_b$) of Al 2024 in seawater and in neutral aqueous chloride solutions, on the square root of the scan rate is plotted in Fig. 3.

A linear dependence between $E_b$ and $v^{1/2}$ was found for all chloride concentrations and also for synthetic seawater, as predicted by Eq. (3). The correlation coefficients were better than 0.999. Intercepts and slopes of the lines for each concentration of $Cl^-$ and for synthetic seawater are listed in Table 2.

The plot of $E_b(v = 0)$ vs. $\log(a_{Cl^-})$ is given in Fig. 4. A good straight line with a slope ranging between 0.145 and 0.156 (values greater than $0.059/\alpha$ (V $dec^{-1}$)) and an intercept of −0.732 V vs. SCE, were obtained. From the experimental slopes values of $\alpha$ between 0.41 and 0.38 were computed.

The average value of the slopes given in Table 2 (0.372), when analysed in terms of Eq. (3), yields a value of 3.29 for $(\xi/J_m)$. With an average value of the steady-state current of 500 μA $cm^{-2}$ and $\chi = 3$, from Eq. (3) a value of $1 \times 10^{15}$ $cm^{-2}$ $s^{-1}$ is obtained for $J_{ca}$. Thus, $J_m \gg 1 \times 10^{15}$ $cm^2$ $s^{-1}$, and, hence, $\xi$ less than or equal to $3 \times 10^{15}$ cation vacancies $cm^{-2}$, which seems to be a very good value.

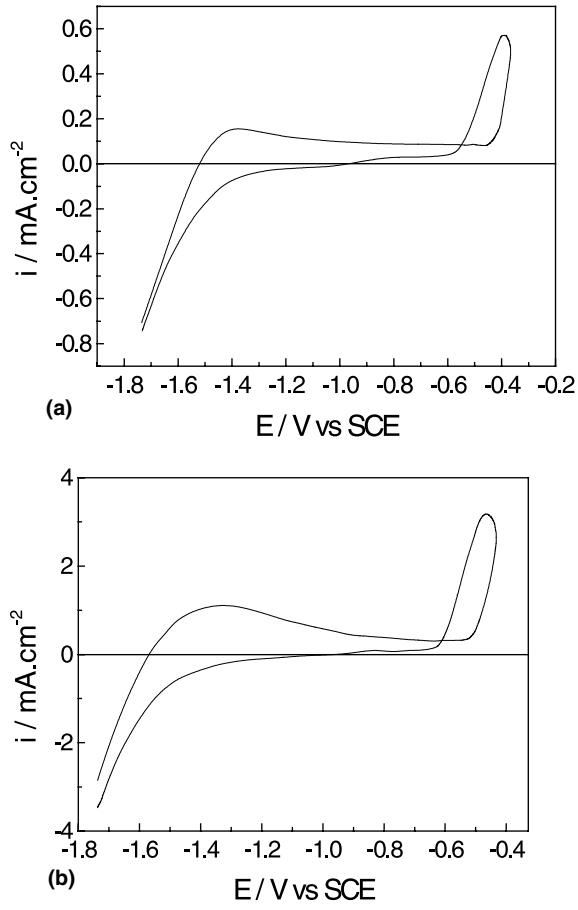


Fig. 2. Cyclic voltammograms of Al 2024-T3 samples in deareated neutral aqueous solutions of sodium chloride. $v = 0.100$ V $s^{-1}$. (a) [NaCl] = 0.05 mol $dm^{-3}$ (b) [NaCl] = 0.5 mol $dm^{-3}$.

In fact, from geometric arguments the number of Al atoms (ions) per unit area on Al and on γ-$Al_2O_3$ can be calculated taking the unit cell dimensions of 4.094 and $7.90 \times 10^{-8}$ cm, respectively. The average number of Al atoms (ions) in a monolayer per unit area computed was 2.4 and $3.4 \times 10^{15}$ $cm^{-2}$, respectively for the Al and $Al_2O_3$ surfaces.

Therefore, our data is a good support of the PDM: data and theory treated independently, without any adjustable parameters, yield the correct value for the density of atoms on the surface.

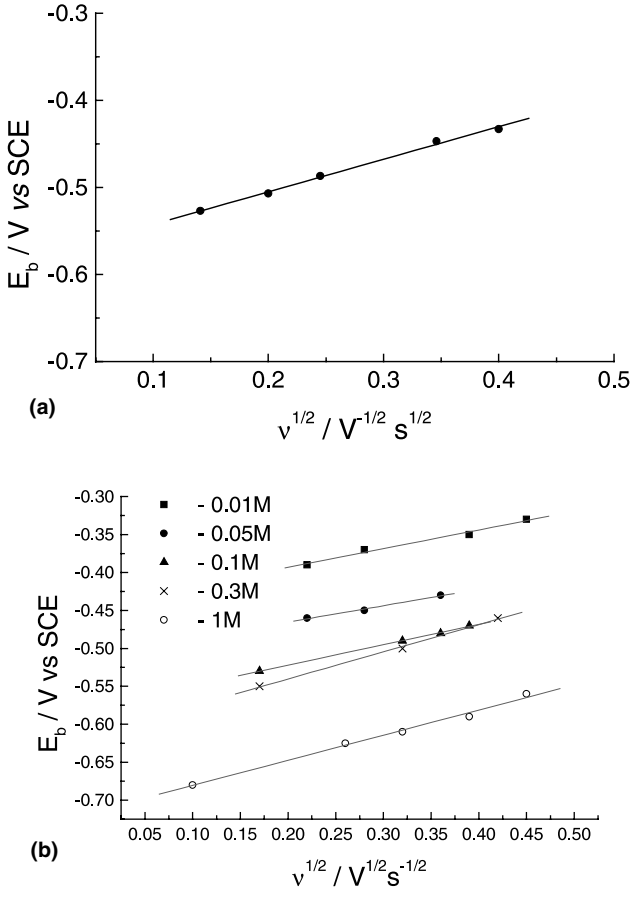


Fig. 3. Plots of $E_b$ vs. $v^{1/2}$ for: (a) Al 2024-T3/synthetic seawater and (b) Al 2024-T3/deaerated aqueous solution of NaCl 0.01; 0.05; 0.1; 0.3 and 1 mol dm$^{-3}$.

Table 2
Parameters from the regression analysis of the $E_b$ vs. $v^{1/2}$ plots of Fig. 3

| [NaCl]/mol dm$^{-3}$ | $E_b(v=0)$/ V vs. SCE | $\partial E_b/\partial v^{1/2}$ ($V^{1/2}$ s$^{-1/2}$) |
|---|---|---|
| 0.01 | −0.442 | 0.246 |
| 0.05 | −0.509 | 0.216 |
| 0.1 | −0.576 | 0.269 |
| 0.3 | −0.644 | 0.552 |
| 0.5 | −0.693 | 0.606 |
| 1 | −0.715 | 0.342 |
| Seawater 0.55 | −0.580 | 0.374 |

## 4. Conclusions

The dependence of the breakdown potential on the potential scan rate, and of the breakdown potential, at zero scan rate, and the logarithm of the activity of the aggressive anions have lead to $\alpha$ values between 0.41 and 0.38 and to a value for $\xi$, less than or equal to $3 \times 10^{15}$ cation cm$^{-2}$.

The average critical concentration of cation vacancies at the metal film interface leading to passivity breakdown, determined from sweep rate dependence of the pitting potential and calculated from structural arguments were in excellent agreement.

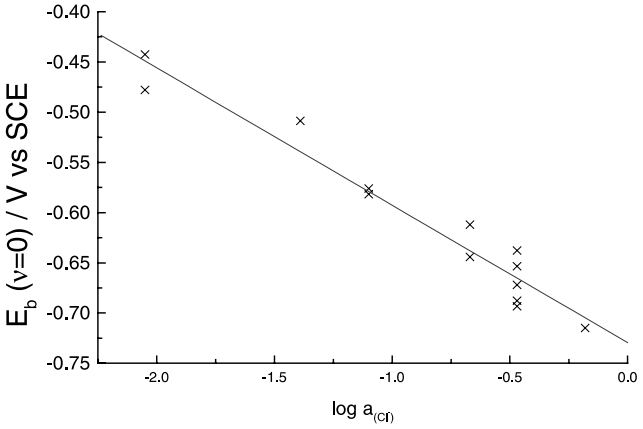


Fig. 4. Plot of $E_b(v=0)$ as a function of the logarithm of the chloride activity.

Data and theory treated independently, without any adjustable parameters, yield the correct value for the density of atoms on the surface. Therefore, our data is a good support of the PDM.

## Acknowledgements

We gratefully acknowledge a number of exchanges of information and discussion with Professor Digby Macdonald.

Fundação para a Ciência e Tecnologia (FCT) from Portugal is also acknowledged for providing financial support to Project PRAXIS-XXI 3/3.1/1919/95 and to CECUL and CCMM research centres.

N. Lima thanks FCT for her grant (PRAXIS BIC/22317/99).

## References

[1] K. Kowal, J. DeLuccia, J.Y. Josefowicz, C. Laired, G. Farrington, J. Electrochem. Soc. 143 (1996) 2471.
[2] R.M. Rynders, C.-H. Paik, R. Lee, C. Alkire, J. Electrochem. Soc. 141 (1994) 1439.
[3] T. Shibata, T. Takeyama, Corrosion 33 (1977) 243.
[4] H. Sato, T. Sato, G. Okamoto, Corros. Sci. 19 (1979) 693.
[5] T. Shibata, Corros. Sci. 52 (1996) 813.
[6] D.E. Williams, C. Westcott, M. Fleischmann, J. Electroanal. Chem. 180 (1984) 549.
[7] D.E. Williams, C. Westcott, M. Fleischmann, J. Electrochem. Soc. 132 (1985) 1796.
[8] D.E. Williams, J. Stweart, P.H. Balkwill, Corros. Sci. 36 (1994) 1213.
[9] R.J. Galvele, Corros. Sci. 21 (1981) 551.
[10] J. Czachor, J. Electrochem. Soc. 128 (1981) 513C.
[11] J. Czachor, C. Wood, G.E. Thompsom, Br. Corros. Sci. 15 (1980) 154.
[12] L.F. Lin, C.Y. Chao, D.D. Macdonald, J. Electrochem. Soc. 128 (1981) 1187.

[13] L.F. Lin, C.Y. Chao, D.D. Macdonald, J. Electrochem. Soc. 128 (1981) 1194.
[14] K.-S. Lei, D. Macdonald, B.G. Pound, B.E. Wilde, J. Electrochem. Soc. 135 (1988) 1625.
[15] D.D. Macdonald, M.U. Macdonald, J. Electrochem. Soc. 137 (1990) 2395.
[16] D.D. Macdonald, J. Electrochem. Soc. 139 (1992) 3434.
[17] T. Haruna, D.D. Macdonald, J. Electrochem. Soc. 144 (1997) 1574.
[18] Patrik Schmuki, Solid State Electrochem. (in press).
[19] D.D. Macdonald, Pure Appl. Chem. 71 (1999) 951.
[20] D.D. Macdonald, D.F. Heaney, Corros. Sci. 42 (2000) 1779.
[21] G. Sussek, M. Kesten, Corros. Sci. 15 (1975) 225.
[22] G.S. Frankel, J. Electrochem. Soc. 145 (1998) 2186.